

# Preparation of strontium-based fibers via electrospinning technique

Nawin Viriya-empikul<sup>\*</sup>, Pattraporn Changsuwan, Kajornsak Faungnawakij

National Nanotechnology Center (NANOTEC), National Science and Technology Development Agency (NSTDA), 111 Thailand Science Park,  
Paholyothin Rd., Patumthani 12120, Thailand

Received 31 August 2011; received in revised form 9 November 2011; accepted 10 November 2011

Available online 20 November 2011

## Abstract

The Sr-based fiber was prepared by electrospinning process. The effect of electric field, precursor viscosity, and calcination temperature ( $T_{\text{cal}}$ ) was investigated at required conditions. Then the Sr-based fiber was characterized by TGA, nitrogen adsorption, SEM, TEM, and XRD to elucidate thermal transition, specific surface area, morphology, crystal structure, and crystalline phase of the samples, respectively. The result showed that the smooth fiber sample could be spun at electric field of  $1.5 \text{ kV cm}^{-1}$  with the suitable viscosity of ca.  $5 \text{ Pa s}$ . Finally the crystalline phase could be controlled by properly adjusting  $T_{\text{cal}}$ , i.e. when the  $T_{\text{cal}}$  was risen from 400 to  $1000^\circ\text{C}$ , the crystalline phase was transformed from  $\text{SrCO}_3$  to  $\text{Sr(OH)}_2\cdot\text{H}_2\text{O}$ , and eventually to  $\text{SrO}$ .

© 2011 Elsevier Ltd and Techna Group S.r.l. All rights reserved.

**Keywords:** Strontium derived; Nanofiber; Electrospin

## 1. Introduction

Strontium belongs to a group of elements known as the alkali earth metals. By chemical reaction, strontium is more active than calcium or magnesium and easily reacts with both air and water [1]. Mostly, strontium has made compound materials (e.g.  $\text{SrO}$ ,  $\text{SrCO}_3$ , and  $\text{Sr(OH)}_2$ ) that are applied to fuel production catalysts [2,3], paint additives [4], and television tubes [5–7]. Recently, the micro and nano-size of strontium compound have been required in chemical and electronic industry [8]. Comparing with large particles (several micron), the small strontium compound particles (nano to sub-micron) have exhibited significantly unusual physical and chemical properties because of their extremely small size and large specific surface area [9]. Therefore the size of particles has been controlled by the synthesis method such as precipitation [10,11], hydrothermal [12,13], solvothermal [14,15], ultrasonic [6] and so on. The best of our knowledge, a fiber-shaped strontium compound has never been synthesized by any techniques before. By electrospinning which is one of the famous techniques to fabricate micro- or nano-fibrous ceramic structure, the electrospun metal compound fibers have been prepared by simply mixing the prior obtained metal salt (e.g.

$\text{Ag-}$ ,  $\text{Ru-}$ ,  $\text{Co-}$ ,  $\text{Pd-}$ ,  $\text{Rh-}$ , and  $\text{Pt-}$ salts) with viscous spinning solution of polymer carriers, for example, poly(ethylene oxide) (PEO), poly(vinyl alcohol) (PVA), poly(acrylic acid) (PAA), and poly(vinylpyrrolidone) (PVP), have been much focused because of their variety of applications, such as textiles, filters, and catalyst [15–18].

In this work, the synthesis of Sr-based fiber via electrospinning technique was proposed. The effect of water ratio (i.e. viscosity) and calcination temperature was discussed on the degradation temperature, morphology, specific surface area, and crystalline phase.

## 2. Experimental

### 2.1. Material and electrospinning preparation

Strontium nitrate ( $\text{Sr(NO}_3)_2$ ) and poly(vinylpyrrolidone) (PVP, K90, MW = 3,600,000) was purchased from Himedia Laboratories Pvt. Ltd. and Fluka Analytical, respectively. The precursor was prepared by mixing of 2g- $\text{Sr(NO}_3)_2$  and 2g-PVP into 6–10 mL water. The mixture was stirred at  $30^\circ\text{C}$  for 8 h or until cleared solution was achieved. Then the precursor was loaded into a 20 mL glass-syringe attached with syringe needle, 22-gauge stainless steel, 12 in. long (Sigma–Aldrich, Z116157). The electrospinning technique was employed by high voltage power which was set at 15 kV. The electric laid between the needle and target (aluminium foil, sized  $7 \text{ cm} \times 7 \text{ cm}$ ) was

<sup>\*</sup> Corresponding author. Tel.: +66 2 564 7100x6570.

E-mail address: [nawin@nanotec.or.th](mailto:nawin@nanotec.or.th) (N. Viriya-empikul).

pinched and manipulated at the electric field of  $1.5 \text{ kV cm}^{-1}$ . Thereafter the liquid flow rate was controlled by syringe pump at  $1 \text{ mL h}^{-1}$ . Finally, the Sr-based fiber was collected and calcined (holding time 5 h) under atmosphere at required temperature ( $400\text{--}1000 \text{ }^{\circ}\text{C}$ ) with a heating rate of  $10 \text{ }^{\circ}\text{C min}^{-1}$ .

## 2.2. Material characterization

The viscosity of each precursor was measured by Rotational Rheometer (Gemini 200 HR Nano, Malvern, UK). The Sr-based fiber was analyzed by thermo-gravimetric/differential thermal analyzer (TGA/SDTA 851<sup>e</sup>, Mettler Toledo, Switzerland) under air flow condition with a ramping rate of  $10 \text{ }^{\circ}\text{C min}^{-1}$  to find out thermal transition of the samples. The crystalline phases of calcined samples were analyzed by X-ray diffraction (JDX-3530, JEOL, Japan) coupled with Cu K $\alpha$  radiation source and accelerated at 30 mA and 40 kV. The Sr-based fibers before and after calcination were characterized by scanning electron microscope (SEM, S-3400, HITACHI, Japan), transmission electron microscope (TEM, JEOL JEM-2010, Japan) and nitrogen adsorption (BELSORP-max, BEL, Japan) to observe their morphology, crystal structure and BET (Brunauer–Emmett–Teller) surface area ( $S_{\text{BET}}$ ), respectively.

## 3. Results and discussion

### 3.1. Preliminary experimental

The preliminary study of this work was provided with the investigation of type of solvent (ethanol and water), electric field ( $1\text{--}2.5 \text{ kV cm}^{-1}$ ), and spinning direction (vertical and horizon). According to the type of solvent, as general knowledge, the polymer (PVP) is well dissolved in ethanol, while strontium nitrate is well dissolved in water. However, strontium nitrate could not be dissolved in ethanol or ethanol aqueous solution (i.e. the precipitation occurred when the ethanol solution was introduced). Therefore, the problem was solved by using water as the solution and spending longer time for dissolving the mixture. For the electric field effect, the Sr-based fiber could not be spun, at low electric field ( $<1 \text{ kV cm}^{-1}$ ), i.e. the cone-shape jet of solution at the syringe tip did not occur. On the other hand, at the electric field above  $2 \text{ kV cm}^{-1}$ , the cone-shape jet could not also be maintained at the needle tip; namely most of the products were agglomerated at the tip due to the high electric force pulling. On the effect of the spinning direction, the obtained fibers of both vertical and horizontal conditions were nearly similar, except that there were some solution drops on the target during the electrospinning process on vertical direction. It could be remarked that the cleared precursor could be prepared in water solvent and spun by applying the electric field of  $1.5 \text{ kV cm}^{-1}$  with the horizontal direction as the optimal conditions which will be employed for the next study.

### 3.2. Effect of water amount (viscosity)

The precursor viscosity ( $\mu$ ) as prepared in the preliminary section for the electrospinning process was measured by

Rotational Rheometer. The water amount was varied from 6 to 10 mL, corresponding with viscosity of the precursor denoted as  $\mu_6$  to  $\mu_{10}$ , respectively. By viscosity comparison, the Newtonian region, i.e. the region that viscosity is independent of shear rate, was found out by plotting the logarithm of viscosity to logarithm of shear rate of each precursor [19,20]. Then the viscosity of all precursors was calculated (viscosity = shear

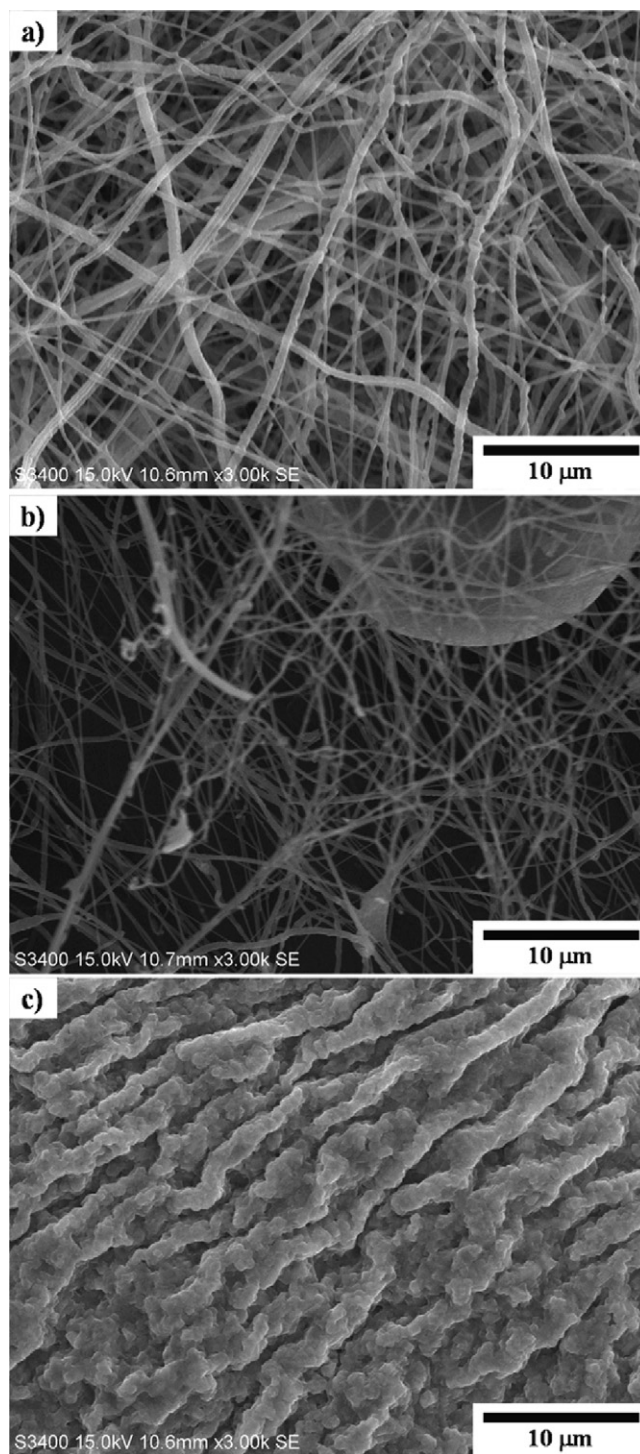


Fig. 1. SEM images of Sr-based fibers spun with electric field of  $1.5 \text{ kV cm}^{-1}$  from precursor having (a)  $\mu = 4.63 \text{ Pa s}$ , (b)  $\mu = 0.98 \text{ Pa s}$ , and (c)  $\mu = 0.41 \text{ Pa s}$ .



stress/shear rate) at the same shear rate of  $2 \text{ s}^{-1}$  in the Newtonian region. The increase of water amount strongly affected the viscosity which is descending shown as follows:  $\mu_6 = 4.63$ ,  $\mu_8 = 0.98$ ,  $\mu_{10} = 0.41 \text{ Pa s}$ .

Regarding the viscosity effect, the result of Sr-based fiber formation was shown in the SEM image (Fig. 1). By the viscosity of  $4.63 \text{ Pa s}$  ( $\mu_6$ ), the cone-shape jet of mixture could withstand during the electrospinning process and thus the formation of Sr-based fiber with the diameter around  $100\text{--}600 \text{ nm}$  was stably attained. On the other hand, the cone-shape jet did not keep stable at the low viscosity ( $\mu_8$  and  $\mu_{10}$ ). Moreover, the decrease in viscosity resulted in the increase in bead formation with a size bigger than  $5 \text{ }\mu\text{m}$  (for  $\mu_8$ ) and shapeless (scale-like) sample (for  $\mu_{10}$ ) as shown in Fig. 1b and c, respectively.

### 3.3. Effect of calcination temperature

The investigation of calcination temperature ( $T_{\text{cal}}$ ) was focused on the selected condition (strontium nitrate:PVP:water =  $2 \text{ g}:2 \text{ g}:6 \text{ mL}$ , electric field of  $1.5 \text{ kV cm}^{-1}$ ) which formed the smooth electrospun fiber. Then the Sr-based fiber calcined under atmosphere at  $400\text{--}1000 \text{ }^\circ\text{C}$  was characterized to find out BET surface area ( $S_{\text{BET}}$ ), morphology, crystal structure, and crystalline phase as revealed in Table 1 and Figs. 2 and 3, respectively. The  $S_{\text{BET}}$  of the sample increased from  $0.4$  (as-synthesized) to  $5\text{--}6 \text{ m}^2 \text{ g}^{-1}$  (calcined) because the polymer matrix was removed. It was confirmed by TG-DTA analysis that the polymer weight dramatically decreased at ca.  $390 \text{ }^\circ\text{C}$  (data not show) suggesting its decomposition temperature. When the  $T_{\text{cal}}$  was raised over  $400 \text{ }^\circ\text{C}$ , the  $S_{\text{BET}}$  of sample decreased due to

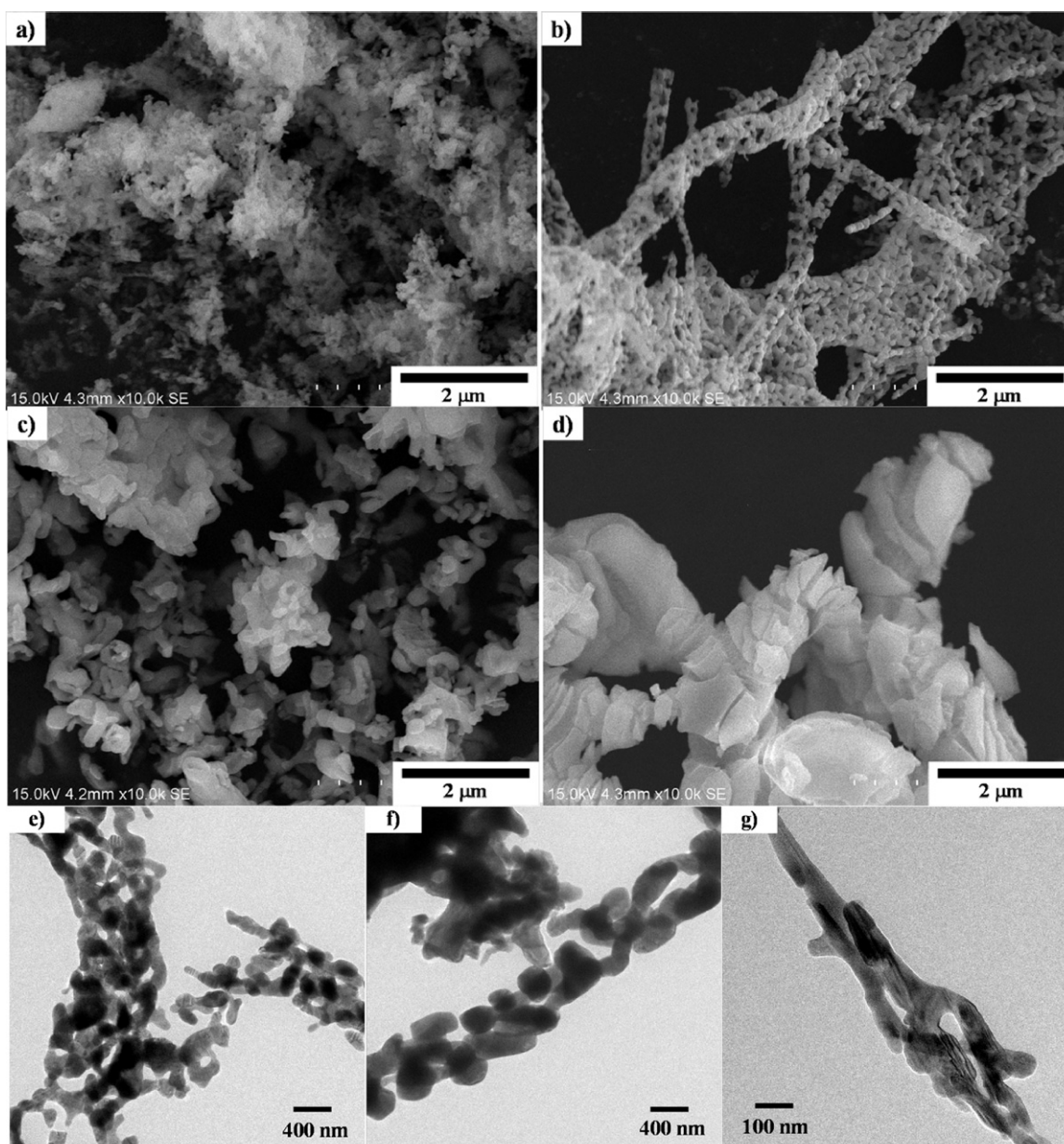


Fig. 2. SEM (a–d) and TEM (e–g) images of calcined Sr-based samples: calcination temperature of (a)  $400 \text{ }^\circ\text{C}$ , (b and e)  $600 \text{ }^\circ\text{C}$ , (c and f)  $800 \text{ }^\circ\text{C}$ , and (d and g)  $1000 \text{ }^\circ\text{C}$ . Electrospinning condition: electric field of  $1.5 \text{ kV cm}^{-1}$  from precursor having  $\mu = 4.63 \text{ Pa s}$ .

Table 1

BET surface area of calcined Sr-based sample spun with electric field of  $1.5 \text{ kV cm}^{-1}$  from precursor having  $\mu = 4.63 \text{ Pa s}$  at required calcination temperature.

|   | Before calcined | 400 °C | 600 °C | 800 °C | 1000 °C |
|---|-----------------|--------|--------|--------|---------|
| SrO fiber ( $\text{m}^2 \text{ g}^{-1}$ ) | 0.4             | 6.8    | 6.0    | 5.2    | Trace   |

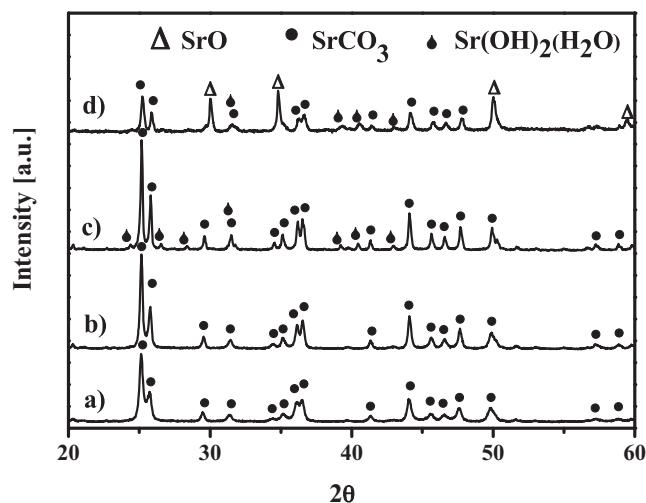


Fig. 3. XRD patterns of calcined Sr-based samples: calcination temperature of (a) 400 °C, (b) 600 °C, (c) 800 °C, and (d) 1000 °C. Electrospinning condition: electric field of  $1.5 \text{ kV cm}^{-1}$  from precursor having  $\mu = 4.63 \text{ Pa s}$ .

the sintering of crystal grain as shown in Fig. 2. At  $T_{\text{cal}}$  of 400 °C, the sponge-like fiber was produced while it still contained some polymer residues. When the polymer in sponge-like fiber was burnt at the  $T_{\text{cal}}$  of 600 °C, the Sr-based particles were agglomerated and formed the porous fiber. The diameter of the fiber ranged from 0.2 to 2  $\mu\text{m}$ , while size of the particles agglomerated to the fibers was in the range of 150–300 nm as shown in Fig. 2b and e. When the  $T_{\text{cal}}$  was higher than 600 °C, the porous fiber (or particle inside the fiber) was sintered and become dense particle and cluster (Fig. 2c, d and f, g). Furthermore, the crystalline phase of the samples was consecutively changed when the calcination temperature increased as illustrated in Fig. 3. Only  $\text{SrCO}_3$  phase occurred at 400–600 °C.  $\text{Sr(OH)}_2\text{H}_2\text{O}$  started to occur at 800 °C, and the mix phases of  $\text{SrO}$ ,  $\text{SrCO}_3$ , and  $\text{Sr(OH)}_2\text{H}_2\text{O}$  occurred at 1000 °C.

#### 4. Conclusions

The synthesis of Sr-based fiber via electrospinning techniques was proposed. The effects of synthesis parameters, including electric field of the electrospinning ( $1.0\text{--}2.5 \text{ kV cm}^{-1}$ ), water amount of the starting material (6–10 mL; viscosity ranged from 4.63 to 0.41 Pa s), and calcination temperature of the as-spun samples, on the fiber formation were systematically studied. The optimal synthesis condition of the Sr-based fiber was observed at electric field of  $1.5 \text{ kV cm}^{-1}$  and viscosity of 4.63 Pa s while the spinning direction was set horizontal. The electrospun fibers provided BET surface areas in the range of  $5\text{--}6 \text{ m}^2 \text{ g}^{-1}$  and

diameter of 200 nm to 2  $\mu\text{m}$  when they were calcined in the temperature range of 600–800 °C. The crystalline phase was sequentially transformed from  $\text{SrCO}_3$  to the mixture of  $\text{SrCO}_3$  and  $\text{Sr(OH)}_2\text{H}_2\text{O}$  (800 °C) and to the mixture of  $\text{SrCO}_3$ ,  $\text{Sr(OH)}_2\text{H}_2\text{O}$  and  $\text{SrO}$  (1000 °C).

#### Acknowledgement

Authors acknowledged the NANOTEC, NSTDA, for financial support to the project P-11-00402.

#### References

- [1] K. Salazar, M.K. McNutt, Mineral Commodity Summaries 2010, U.S.G.S. Department of the Interior, United States Government Printing Office, Washington, DC, 2010.
- [2] B. Yoosuk, P. Krasae, B. Puttasawat, P. Udomsap, N. Viriya-empikul, K. Faungnawakij, Magnesia modified with strontium as a solid base catalyst for transesterification of palm olein, *Chem. Eng. J.* 162 (2010) 58–66.
- [3] K. Omata, N. Nukui, T. Hottai, Y. Showa, M. Yamada, Strontium carbonate supported cobalt catalyst for dry reforming of methane under pressure, *Catal. Commun.* 5 (2004) 755–758.
- [4] S. Li, H. Zhang, J. Xu, D. Yang, Hydrothermal synthesis of flower-like  $\text{SrCO}_3$  nanostructures, *Mater. Lett.* 59 (2005) 420–422.
- [5] T.J. Bastow, Electric field gradients at the M-site in  $\text{MCO}_3$ : M = Mg, Ca, Sr and Ba, *Chem. Phys. Lett.* 354 (2002) 156–159.
- [6] M.A. Alavi, A. Morsali, Syntheses and characterization of  $\text{Sr(OH)}_2$  and  $\text{SrCO}_3$  nanostructures by ultrasonic method, *Ultrason. Sonochem.* 17 (2010) 132–138.
- [7] J. Du, Z. Liu, Z. Li, B. Han, Y. Huang, J. Zhang, Synthesis of mesoporous  $\text{SrCO}_3$  spheres and hollow  $\text{CaCO}_3$  spheres in room-temperature ionic liquid, *Micropor. Mesopor. Mater.* 83 (2005) 145–149.
- [8] J. Yu, H. Guo, B. Cheng, Shape evolution of  $\text{SrCO}_3$  particles in the presence of poly-(styrene-alt-maleic acid), *J. Solid State Chem.* 179 (2006) 800–803.
- [9] D.H. Chen, Y.Y. Chen, Synthesis of strontium ferrite nanoparticles by coprecipitation in the presence of polyacrylic acid, *J. Mater. Res.* 37 (2002) 801–810.
- [10] F.A. Rabuffetti, P.C. Stair, K.R. Poeppelmeier, Synthesis-dependent surface acidity and structure of  $\text{SrTiO}_3$  nanoparticles, *J. Phys. Chem. C* 114 (2010) 11056–11067.
- [11] C.F. Kao, C.L. Jeng, Preparation and characterisation of lanthanum nickel strontium oxides by combined coprecipitation and molten salt reactions, *Ceram. Int.* 26 (2000) 237–243.
- [12] S. Ni, X. Yang, T. Li, Hydrothermal synthesis and photoluminescence properties of  $\text{SrCO}_3$ , *Mater. Lett.* 65 (2011) 766–768.
- [13] J. Zhao, X. Wang, L. Li, X. Wang, Y. Li, Stoichiometry control and structure evolution in hydrothermally derived (Ba,Sr) $\text{TiO}_3$  films, *Ceram. Int.* 34 (2008) 1223–1227.
- [14] L. Shi, F. Du, Solvothermal synthesis of  $\text{SrCO}_3$  hexahedral ellipsoids, *Mater. Lett.* 61 (2007) 3262–3264.
- [15] N. Sangkhaoprom, P. Supaphol, V. Pavarajarn, Fibrous zinc oxide prepared by combined electrospinning and solvothermal techniques, *Ceram. Int.* 36 (2010) 357–363.
- [16] A. Mahapatra, B.G. Mishra, G. Hota, Synthesis of ultra-fine  $\alpha\text{-Al}_2\text{O}_3$  fibers via electrospinning method, *Ceram. Int.* 37 (2011) 2329–2333.
- [17] J. Kaewsanee, P. Visal-athaphand, P. Supaphol, V. Pavarajarn, Fabrication and characterization of neat and aluminium-doped titanium (IV) oxide fibers prepared by combined sol-gel and electrospinning techniques, *Ceram. Int.* 36 (2010) 2055–2061.
- [18] S. Wannapop, T. Thongtem, S. Thongtem, Characterization of  $\text{SrWO}_4$ -PVA and  $\text{SrWO}_4$  spiders' webs synthesized by electrospinning, *Ceram. Int.* (2011).
- [19] T.G. Mezger, *The Rheology Handbook: For Users of Rotational and Oscillatory Rheometer*, second ed., Hannover, Germany, 2006.
- [20] L.A. Utracki, *Polymer Blends Handbook*, vol. 1, Dordrecht, The Netherlands, 2002.